



Original

Schisandrin ameliorates cognitive deficits, endoplasmic reticulum stress and neuroinflammation in streptozotocin (STZ)-induced Alzheimer's disease rats

Lin SONG¹⁾, Zhongyuan PIAO²⁾, Lifen YAO³⁾, Limei ZHANG⁴⁾ and Yichan LU⁵⁾

¹⁾School of Life Sciences, Huizhou University, 46 Yanda Avenue, Huizhou, Guangdong 516007, P.R. China

²⁾Department of Neurology, Huizhou Third People's Hospital, Huizhou Hospital of Guangzhou Medical University, 1 Xuebei Street, Huizhou, Guangdong 516002, P.R. China

³⁾Department of Neurology, The First Affiliated Hospital of Harbin Medical University, 23 Youzheng Street, Harbin, Heilongjiang 150001, P.R. China

⁴⁾Department of Obstetrics and Gynecology, Huizhou Third People's Hospital, Huizhou Hospital of Guangzhou Medical University, 1 Xuebei Street, Huizhou, Guangdong 516002, P.R. China

⁵⁾Department of Chinese Medicine, Dalian Maternity and Child Health Care Hospital, 321 Jiefang Road, Dalian, Liaoning 116033, People's Republic of China

Abstract: Schisandrin, an active component extracted from *Schisandra chinensis* (Turcz.) Baill has been reported to alleviate the cognitive impairment in neurodegenerative disorder like Alzheimer's disease (AD). However, the mechanism by which schisandrin regulates the cognitive decline is still unclear. In our study, intracerebroventricular injection of streptozotocin (STZ) was employed to establish AD model in male Wistar rats, and indicated dose of schisandrin was further administered. The Morris water maze test was performed to evaluate the ability of learning and memory in rats with schisandrin treatment. The results indicated that schisandrin improved the capacity of cognition in STZ-induced rats. The contents of pro-inflammatory cytokines in brain tissue were determined by ELISA, and the expressions of these cytokines were assessed by western-blot and immunohistochemistry. The results showed that treatment of schisandrin significantly reduced the production of inflammation mediators including tumor necrosis factor- α , interleukin-1 β and interleukin-6. Further study suggested a remarkable decrease in the expressions of ER stress maker proteins like C/EBP-homologous protein, glucose-regulated protein 78 and cleaved caspase-12 in the presence of schisandrin, meanwhile the up-regulation of sirtuin 1 (SIRT1) was also observed in the same group. Additionally, the results of western-blot and EMSA demonstrated that schisandrin inhibited NF- κ B signaling in the brain of STZ-induced rats. In conclusion, schisandrin ameliorated STZ-induced cognitive dysfunction, ER stress and neuroinflammation which may be associated with up-regulation of SIRT1. Our study provides novel mechanisms for the neuroprotective effect of schisandrin in AD treatment.

Key words: Alzheimer's disease, endoplasmic reticulum (ER) stress, neuroinflammation, schisandrin, sirtuin 1 (SIRT1)

Introduction

Alzheimer's disease (AD) is a typical neurodegenerative disorder that mainly occurs among the older people [4, 5]. According to the latest report, approximately 44 million people are suffering from the AD which leads to

an increasingly economic burden for society [4]. The phenotypic characteristics of Alzheimer's disease (AD) are loss of memory, impairment of social behaviors and alterations in personality [4, 8]. This kind of cognitive deficit caused by Alzheimer's disease is always accompanied with the up-regulation of acetylcholinesterase

(Received 18 November 2019 / Accepted 30 March 2020 / Published online in J-STAGE 24 April 2020)

Corresponding author: L. Song. e-mail: drlinsong@163.com



This is an open-access article distributed under the terms of the Creative Commons Attribution Non-Commercial No Derivatives (by-nc-nd) License <<http://creativecommons.org/licenses/by-nc-nd/4.0/>>.

©2020 Japanese Association for Laboratory Animal Science

(AChE) activity, tau phosphorylation and amyloid aggregation [5, 8]. The etiology and pathogenesis of AD are very complex, and some reports have suggested that a variety of biochemical and molecular alteration is involved in the AD pathology, such as the alteration of oxidative stress, impairment of mitochondria and apoptosis [24]. Moreover, some studies find out that chronic neuroinflammatory response induced by activated microglia may be the one of the major etiologies of AD. The activation of microglia leads to the production of pro-inflammatory cytokines which induces the chronic inflammatory response and partly mediates the neuronal death and synaptic impairment in AD [24]. The endoplasmic reticulum (ER) stress is also regarded as another significant factor leading to the occurrence of AD. The amassment of misfolded protein and dysregulation of Ca^{2+} signaling are considered to induce the ER stress and cause the dysfunction of neuronal and cell death [10].

Schisandrin is an active component extracted from the fruit of *schisandra chinensis* Baill [34], and it has been reported to function in various diseases. Positive involvement of schisandrin is demonstrated in MPTP-induced Parkinson's disease [33], breast cancer [30], and Alzheimer's disease [21]. As a traditional medicine, schisandrin possesses various pharmacological properties, such as anti-oxidative activity and anti-inflammation. Schisandrin can repress the microglia-induced neuroinflammation via inhibiting the NF- κ B and JAK-STAT3 pathway [33]. In addition, schisandrin can also function as the activator of sirtuin 1 (SIRT1), a member of the class II histone deacetylase family. It has been proved that STRT1 plays an important role in regulating inflammation and endoplasmic reticulum stress [31]. However, the comprehensive identification whether schisandrin negatively mediates the neuroinflammation and endoplasmic reticulum stress by regulating STRT1 is still unclear.

In our study, we aim to figure out whether schisandrin ameliorates the neuroinflammation and ER stress in streptozotocin (STZ) induced AD model and enrich the therapeutic effect of schisandrin.

Material and Methods

Animals

Male Wistar rats (3–4 months old) weighing 300–400 g were purchased from Animal Experimental Center of Harbin Medical University (Harbin, China). Animals were maintained with enough food and water on a 12/12 h light/dark circle under the temperature of $25 \pm 1^\circ\text{C}$ and humidity of 45–55%. There are at least 6 rats in each

group. The experiments were approved by the Animal Ethics Committee of the First Affiliated Hospital of Harbin Medical University and all efforts were made to minimize the number of animals and their suffering.

Drugs and antibodies

STZ (purity $\geq 98\%$) was purchased from Aladdin reagents Co., Ltd., Shanghai, China. Schisandrin (Sch) (purity $\geq 98\%$) was purchased from Dalian Melun Biotechnology Co., Ltd., Dalian, China. TNF- α antibody (17590-1-AP), CHOP antibody (15204-1-AP), SIRT1 antibody (13161-1-AP), NF- κ B antibody (14220-1-AP) and reference antibody GAPDH (60004-1-Ig) were purchased from Proteintech Inc. (Wuhan, China). IL-1 β antibody (A1112), IL-6 antibody (A0286) and GRP78 antibody (A0241) were purchased from ABclonal (Wuhan, China). Cleaved caspase-12 antibody (GTX59923) and reference antibody Histone H3 (GTX122148) were purchased from Gene Tex (Irvine, CA, USA). I κ B α (AF5002), p-I κ B α (AF2002) and IKK α/β (AF6014) antibodies were purchased from Affinity (Beijing, China). p-IKK α/β antibody (#2697) was purchased from Cell Signaling Technology (Danvers, MA, USA). Goat anti rabbit IgG (SE134) and goat anti mouse IgG (SE131) were purchased from Solarbio Science & Technology (Beijing, China).

Establishment of AD model and drug treatment

Rats were randomly divided into four groups ($n=6$ per group): control, STZ, STZ with low dose of Sch (Sch+L), STZ with high dose of Sch (Sch+H). The STZ groups with or without Sch treatment were administrated with bilateral intracerebroventricular (ICV) injections of STZ (3 mg/kg total dose) diluted in sterile 0.9% saline (4.5 μ l for a single injection). The control group was injected with the same volume of sterile 0.9% saline. Two weeks after the treatment of STZ, the schisandrin treated groups were separately administrated with indicated dose of Sch for 2 weeks (2 mg/kg/d or 4 mg/kg/d) by intraperitoneal injection. The control and the STZ treated group were intraperitoneally received the same volume of sterile 0.9% saline. After the treatment of schisandrin, some of the rats were sacrificed and others were used for Morris water maze test. Brains were collected and rinsed with ice-cold PBS (0.01 M, pH 7.4) to get rid of the excess blood. The brain tissues were stored at -80°C .

Morris water maze test

The Morris water maze (MWM) test was performed to assess whether schisandrin treatment could alleviate the impairment of learning and memory in AD rats. The Morris water maze is a stainless-steel circular water tank

(120 cm diameter×50 cm in height) with a platform (10 cm diameter) setting in the second quadrant, and the distance below the water surface is 1cm. The temperature of the water was set at $25 \pm 1^\circ\text{C}$. For navigation test, it was conducted twice a day for five continuous days. Firstly, the rats were placed in the water facing the wall of pool, and allowed to explore the hidden platform within 90 s. The escape latency was recorded when the rats succeed in finding the platform and stayed on it for 2 s. If the rats did not find the platform within 90 s, the latency was recorded as 90 s and the rats were guided to the platform and stayed there for 15 s. The probe trial was performed 24 h after the last training for the navigation test, the platform was taken away and the rats were placed in the water facing the wall of pool and allowed to search for the platform freely for 90 s. The number of platform position crossings was recorded.

ELISA

Tissue samples (100 mg) were homogenized with PBS at the ratio of 1:9, and then centrifuged at 430 g for approximately 10 min at 4°C , and the supernatants were used for ELISA quantification. The experiments were performed according to the manual instructions (Multi-Sciences Biotech Co., Ltd., Hangzhou, China). The ELISA assay was measured at 450 nm and the results are expressed as pg/ml of total protein.

Western-blot analysis

The RIPA lysis buffer comprises of 50 mM Tris-HCl, 300 mM NaCl, 0.5% TritonX-100, and 5 mM EDTA. The brain tissues were dissociated with indicated RIPA containing PMSF with the final concentration of 1 mM on ice for 5 min and then centrifuged at 10,000 g for 5 min at 4°C . The supernatants were collected and the total protein was measured by BCA protein quantification kit (PC0020, Solarbio Science & Technology, Beijing, China). The nuclear and cytoplasmic proteins were extracted by nuclear protein extraction kit (R0050, Solarbio Science & Technology). Protein samples were loaded on SDS-polyacrylamide electrophoresis gels, transferred onto polyvinylidenedifluoride (PVDF) membranes, and blocked with 5% skim milk in Tris buffered saline-Tween20 (TBST). The membranes were incubated with primary antibodies; rabbit anti-TNF- α (1:500, Proteintech), rabbit anti-IL-6 (1:1,000, Abclonal), rabbit anti-IL-1 β (1:500, Abclonal), rabbit anti-GRP78 (1:1,000, Abclonal), rabbit anti-cleaved caspase-12 (1:200, GeneTex), rabbit anti-CHOP (1:500, Proteintech), rabbit anti-SIRT1 (1:500, Proteintech), rabbit anti-I κ B α (1:1,000, Affinity), rabbit anti-p-I κ B α (1:1,000, Affinity), rabbit anti-IKK α/β (1:1,000, Affinity), rabbit

anti-p-IKK α/β (1:1,000, Cell Signaling Technology, Danvers, MA, USA), rabbit anti-NF- κ B (1:1,000, Proteintech), mouse anti-GAPDH (1:10,000, Proteintech) and mouse anti-Histone (1:5,000, GeneTex), overnight at 4°C , then followed by the incubation with the goat against rabbit/mouse HRP-conjugated secondary antibodies (1:3,000, Solarbio Science & Technology) for 1 h at 37°C . The results were visualized by enhanced chemiluminescence (Solarbio Science & Technology) and band intensities of the western blot were analyzed using Gel-Pro-Analyze software.

Immunohistochemistry

The brain tissues were frozen in ethanol and stored at -80°C until sectioning. Tissues were dehydrated in a series of graded alcohols after rinsing with water. The brain tissues were displayed by paraffin-section method. The paraffin sections were dewaxed, rehydrated and then placed in the boiled citrate buffer (10 m mol/ L, pH 6.0) for another 10 min using a microwave oven for antigen retrieval. After that, the sections were incubated with 3% H_2O_2 for 15 min at room temperature to eliminate the activity of endogenous peroxidase. Subsequently, the sections were washed with PBS and blocked with normal goat serum (SL038, Solarbio Science & Technology) for 15 min at room temperature. After the last step, the sections were incubated with the primary rabbit anti-TNF- α (bs-10802R), IL-6 (bs-4539R) and IL-1 β (bs-0812R) antibodies (1:200, BIOSS, Beijing, China) overnight at 4°C . After washing, the sections were incubated in HRP-conjugated goat anti-rabbit IgG (#31460, 1:500, ThermoFisher, Waltham, MA, USA) at 37°C for 1 h followed by the DAB incubation. The sections were redyed with hematoxylin for another 3 min. After dehydration, transparency and sealing, the images were maintained using a microscope (Olympus DP73, Tokyo, Japan).

Immunofluorescence

After the section preparation and antigen retrieval, the sections were washed with PBS and blocked with normal goat serum (SL038, Solarbio Science & Technology) for 15 min at room temperature. Then, the sections were incubated overnight at 4°C with the primary rabbit anti-CHOP (1:200, Proteintech) antibody, mouse anti-GFAP (1:50, Santa Cruz Biotechnology, Santa Cruz, CA, USA) antibody and mouse anti-Iba1 (1:200, Genetex) antibody. After washing, the sections were incubated in Cy3-conjugated and FITC-conjugated secondary antibodies (A0516, A5608, 1:200, Beyotime Biotechnology, Haimen, China) for 1 h at room temperature in the dark. The sections were further treated with DAPI for another 20 min at room temperature. After the washing and seal-

ing, the images were observed using a fluorescence microscope (DP73, Olympus, Tokyo, Japan).

Quantification of SIRT1 activity

The activity of SIRT1 was measured under the guidance of the manual instructions (GMS50287.2, Genmed Scientifics, Shanghai, China).

Real-time quantitative PCR

Real-time PCR was performed to detect the mRNA expression level of *Sirt1* in rat brain tissue. Total RNA was extracted with TRIpure (DP419, Tiangen Biotech, Beijing, China) and the concentration of total RNA was further determined by ultraviolet spectrophotometer (NANO 2000, ThermoFisher). Subsequently, cDNA was obtained by the reverse transcriptase Super M-MLV (NG212, Tiangen Biotech). The following primers were used for real-time PCR:

SIRT1-F: 5'-ATAAATAGGGAACCTCTGCC-3';
 SIRT1-R: 5'-GCTTTACAGGGTTACAACAA-3';
 GAPDH-F: 5'-CGGCAAGTTCAACGGCACAG-3';
 GAPDH-R: 5'-CGCCAGTAGACTCCACGACAT-3';

Real time quantitative PCR was conducted according to the protocol using the SYBR Green (SY1020, Solarbio Science & Technology) on ExicyclerTM96 machine (Bioneer Co, Daejeon, Korea). The data was analyzed and the amount of mRNA was calculated using $2^{-\Delta\Delta CT}$.

Electrophoretic Mobility Shift Assay (EMSA)

For EMSA, biotin-labeled double-stranded NF- κ B motif oligos (5'-AGT TGA GGG GAC TTT CCC AGG C-3') purchased from Beyotime Biotechnology (GS056B) were applied as probe. Nuclear proteins extracted from the brain tissues were evaluated by EMSA to assess their DNA binding activity. The reaction mix was made at the appropriate ratio according to the instruction (GS009, Beyotime Biotechnology) and the probe should be added at the last step. The reaction mix was separated on 6.5% nondenaturing polyacrylamide gel in 0.25 \times TBE pre-cooling buffer. The gel was run on the ice at 180 V for 80 min and it was further transferred onto the nylon membrane, then the DNA was cross-linked by the UV-light cross-linker. Subsequently, the membrane was incubated with the streptavidin-HRP conjugate (1:750, Beyotime Biotechnology) for 20 min at room temperature after blocking and washing. The membrane was then added with ECL (Beyotime Biotechnology) working solution and reacted for 5 min. It was covered with plastic wrap and exposed in the dark room for imaging.

Statistical analysis

All values were expressed as the means \pm SD, statistical analysis was performed using GraphPad Prism. Comparisons between groups were made by using one-way ANOVA followed by Tukey's tests. *P* values of less than 0.05 were considered statistically significant.

Results

Schisandrin ameliorates the impairment of cognition in STZ-induced rats

Cognitive impairment and progressively loss of memory are the most characteristic symptoms of AD, and ICV-injection of STZ successfully simulated the cognitive decline in rats [8]. To investigate whether schisandrin alleviated the STZ-induced cognitive decline in rats, the Morris water maze test was performed to assess the capacity of spatial memory in AD rats with or without schisandrin treatment. We found that the escape latency was much longer in STZ treated rats than that in normal rats, while the treatment of 4 mg/kg of Sch significantly reduced the escape latency of the rats (Fig. 1A). The results of probe trial demonstrated that the numbers of crossing the platform in STZ treated rats were significantly less than that in the control rats, whereas the treatment of Sch increased the frequency of crossing the platform in dose-dependent manner (Fig. 1B), which indicated that Schisandrin could ameliorate the impairment of cognition in STZ-induced rats.

Schisandrin inhibits the STZ-induced neuroinflammation in rats

Neuroinflammation is another significant feature of AD. To determine whether Sch suppressed the neuroinflammation in STZ-induced rats, the secretion of inflammation mediators was measured by the ELISA assay kit. The results indicated that STZ treatment could significantly raise the contents of TNF- α , IL-6 and IL-1 β in brain tissue compared to the normal group, and treatment with Sch could decrease the production of TNF- α , IL-6 and IL-1 β induced by STZ (Figs. 2A–C). Immunoblot analysis and immunohistochemistry were further performed to evaluate the expression levels of these inflammation mediators in the brain tissue. Obvious increased expressions of TNF- α , IL-6 and IL-1 β were observed in the STZ-treated group compared with the normal group, while treatment of schisandrin dose-dependently decreased the expression levels of these pro-inflammatory cytokines (Figs. 2D and E), which indicated that schisandrin alleviated the neuroinflammation in the brain of STZ-induced AD rats.

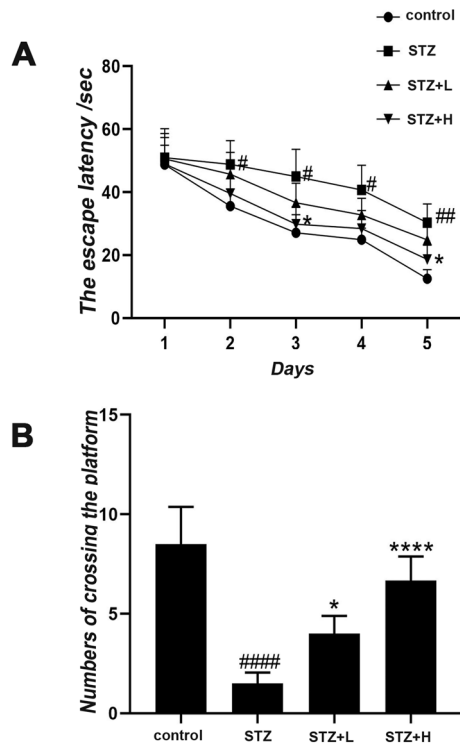


Fig. 1. Schisandrin ameliorates the impairment of cognition in streptozotocin (STZ)-induced rats. (A) The escape latency to find the hidden platform. (B) The number to cross the platform within 60 s. Values are expressed as mean \pm SD. $n=6$. Compared with control group: # $P<0.05$, ## $P<0.01$, ### $P<0.001$, #### $P<0.0001$; Compared with STZ group, * $P<0.05$, ** $P<0.01$, *** $P<0.001$, **** $P<0.0001$.

Schisandrin inhibits STZ-induced endoplasmic reticulum stress in rats

The response of endoplasmic reticulum stress is considered as a momentous process in the etiology of AD. To clarify whether schisandrin inhibited the STZ-induced endoplasmic reticulum stress in AD rats, immunofluorescence staining was performed to detect the expression of C/EBP Homologous Protein (CHOP), an ER stress marker. The results showed that Sch treatment led to obvious attenuation of CHOP against the STZ treatment (Fig. 3A). The results of western-blot in Fig. 3B showed that the expression of CHOP was significantly elevated in the brain of STZ rats while Sch treatment caused remarkable down-regulation of CHOP against STZ rats (Fig. 3B). Western-blot analysis was also performed to detect the expression of glucose-related protein 78 (GRP78) and cleaved caspase-12, and the results indicated that Sch significantly reduced the expressions of these ER stress markers which were up-regulated in STZ rats (Fig. 3C). Actually, we further investigated the cell types in which the schisandrin-induced alleviation of ER stress was arisen. Using the immunochemical markers (GFAP for astrocyte; Iba1 for microglia) for the deter-

mination of brain cell types in rats, we have figured out that staining of CHOP in nucleus (marked with red arrowhead) was found to be surrounded with staining of GFAP, indicating the whole cellular structure of astrocyte. CHOP is present in the cytoplasm under non-stressed conditions and ER stress leads to its nuclear accumulation, while the location of marker protein (GFAP and Iba1) was shown to be cytoplasm in our study. We thus thought that schisandrin-induced alleviation of ER stress was mainly present in astrocyte, while not in microglia (Figs. 3D and E).

Schisandrin enhances the activity of SIRT1 in STZ-treated rats

SIRT1 is attributed to the class II histone deacetylase family which has been confirmed to play an important role in the acquisition and maintenance of memory [7]. To determine whether schisandrin enhanced the activity of SIRT1 in STZ-induced AD rats, western-blot analysis and real-time PCR were firstly performed to evaluate the expression level of SIRT1 in rat brain tissues. As shown in Figs. 4A and B, STZ significantly reduced the expression levels of SIRT1, while treatment of Sch up-regulated the mRNA and protein levels of SIRT1 in the contrast to STZ. As shown in Fig. 4C, STZ treatment significantly reduced the activity of SIRT1 compared with the control, while the treatment of high dose of Sch enhanced activity of SIRT1 compared to the STZ treatment.

Schisandrin restrains the NF- κ B signaling in STZ-induced rats

The nuclear transcription factor (NF- κ B) participates in the mediation of inflammatory response. Results of western-blot showed the degradation of I κ B α and the phosphorylation of I κ B α and IKK α / β in STZ induced group which was reversed after schisandrin treatment (Figs. 5A and B). In addition, significant decrease of NF- κ B in cytoplasm while the augment in nucleus were found after the treatment of STZ, and schisandrin showed the inhibitory effect compared with STZ treatment (Fig. 5C). EMSA was next performed to determine the NF- κ B DNA binding activity, and results in Fig. 5D indicated that schisandrin remarkably inhibited the DNA binding ability to NF- κ B.

Discussion

In the present study, we found the relief of neuroinflammation and ER stress by schisandrin in STZ-induced AD models. Alzheimer's disease is clinically divided into two types including sporadic AD (SAD) and familial AD (FD), and the SAD accounts for 95% of the all

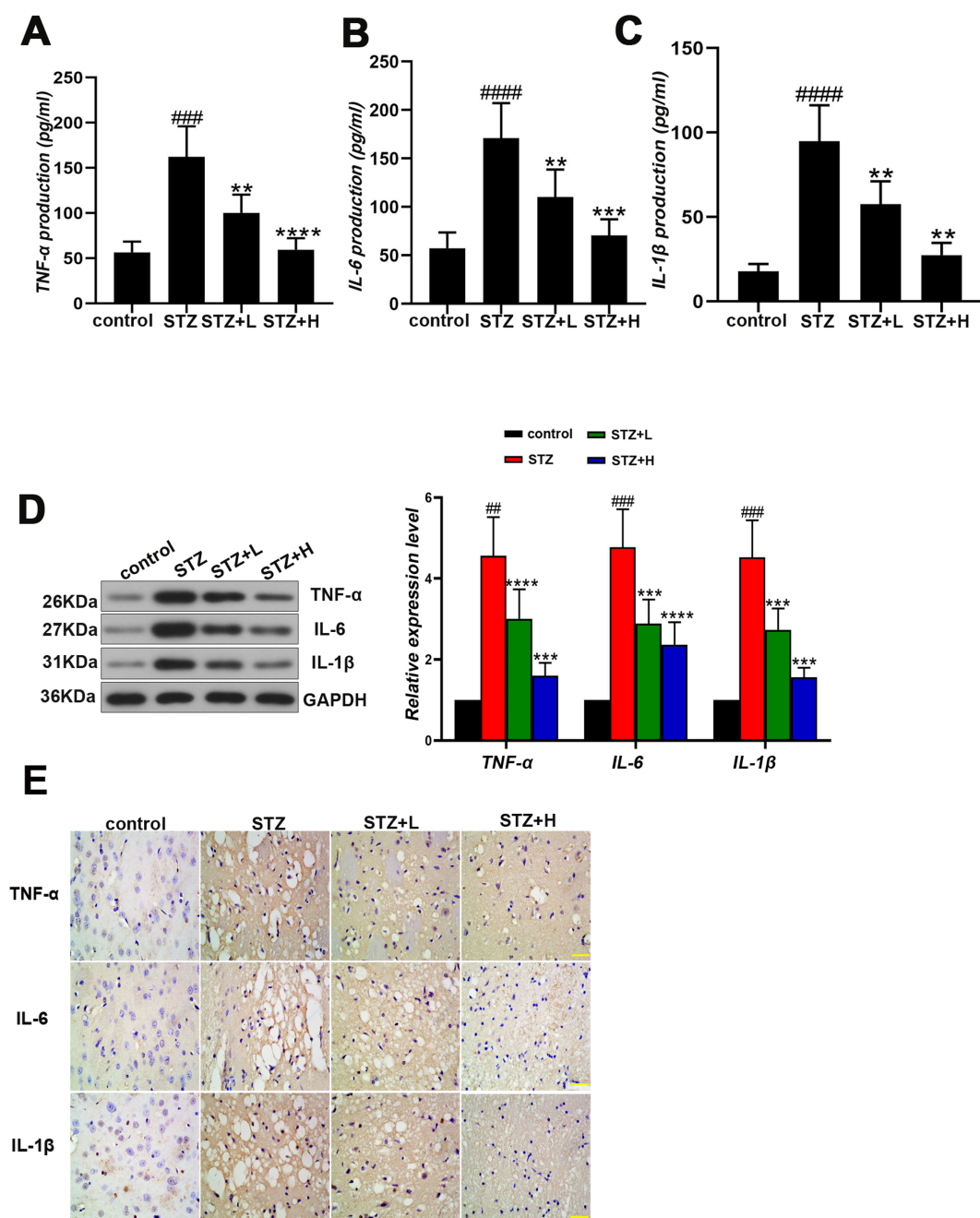


Fig. 2. Schisandrin inhibits the streptozotocin (STZ)-induced neuroinflammation in the brain of rats. Production of TNF- α (A), IL-6 (B) and IL-1 β (C) were detected by ELISA assay kits. (D) The protein expressions of TNF- α , IL-6 and IL-1 β were detected by western-blot. (E) The expressions of TNF- α , IL-6 and IL-1 β were detected by immunohistochemical staining, and changes in the region of cerebral cortex were particularly observed. Scale bar: 50 μ m. Values are expressed as mean \pm SD. n=6. Compared with control group: # P <0.05, ## P <0.01, ### P <0.001, #### P <0.0001; Compared with STZ group, * P <0.05, ** P <0.01, *** P <0.001, **** P <0.0001.

AD cases [16]. Intracerebroventricular (ICV) injection of streptozotocin (STZ) is a universally accepted method to establish the model of sporadic ADs [3, 23]. Pre-clinical studies have found the memory and learning deficits along with the observation of cerebral atrophy, amyloid plaques, and neurofibrillary tangles in STZ-treated rats [13]. Schisandrin has been suggested the potential to exert the neuroprotective effect on Alzheimer's

er's disease [27]. The Morris water maze test was performed in our study after the treatment of schisandrin. The results showed that schisandrin significantly alleviate the decline of memory and learning abilities in STZ rats which indicated the anti-AD effect of schisandrin.

It is known that sporadic AD is widespread with an unclear etiology compared to familial AD with genetic origin. There are varieties of hypotheses to clarify the

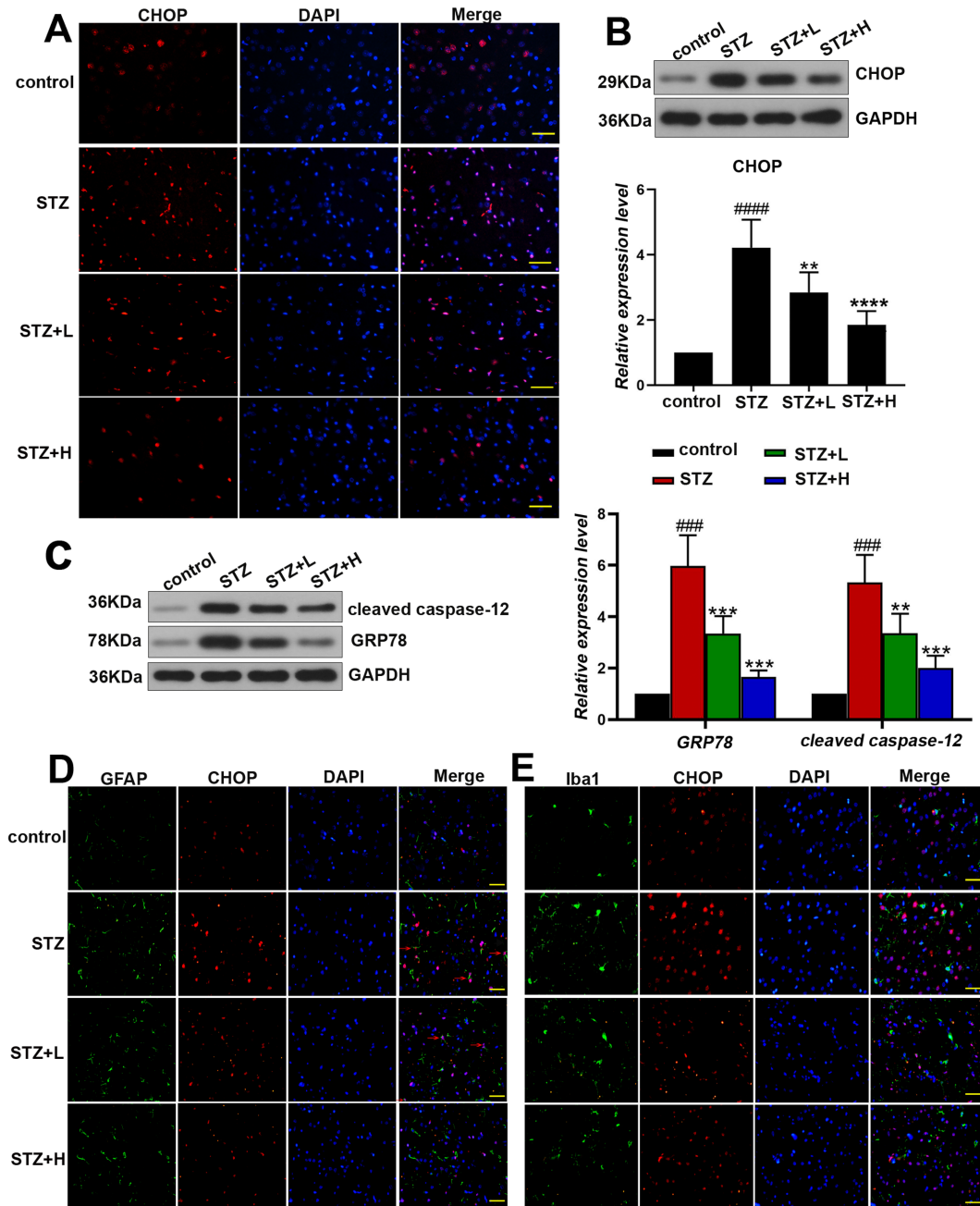


Fig. 3. Schisandrin alleviates streptozotocin (STZ)-induced endoplasmic reticulum stress in the brain of rats. (A) The expression of CHOP was analyzed by immunofluorescence assay, and changes in the region of cerebral cortex were particularly observed. Scale bar: 50 μ m. The protein levels of CHOP (B), GRP78 and cleaved caspase-12 (C) were detected by western-blot. (D) Representative images of double immunofluorescent staining for CHOP and astrocyte marker (GFAP). Scale bar: 50 μ m. (E) Representative images of double immunofluorescent staining for CHOP and microglia marker (Iba1). Scale bar: 50 μ m. Values are expressed as mean \pm SD. n=6. Compared with control group: # P <0.05, ## P <0.01, ### P <0.001, #### P <0.0001; Compared with STZ group, * P <0.05, ** P <0.01, *** P <0.001, **** P <0.0001.

cause of SAD, while the ultimate etiology of SAD remains to explore. In our study, we found that inflammatory response was activated in STZ induced rats. The expressions of pro-inflammatory cytokines including TNF- α , IL-6 and IL-1 β were significantly elevated in AD model. TNF- α is released by lymphocytes, fibroblasts, leukocytes and epithelial cells and functions

mainly by interacting with the Tumor necrosis factor receptors (TNFRs) [2]. TNF- α is a critical pro-inflammatory cytokine which activates the subsequent inflammatory response by triggering various signaling pathways and stimulates the expressions of IL-6 and IL-1 β , these cytokines ultimately resulted in inflammation and activation of NF- κ B [15]. Previous studies have sug-

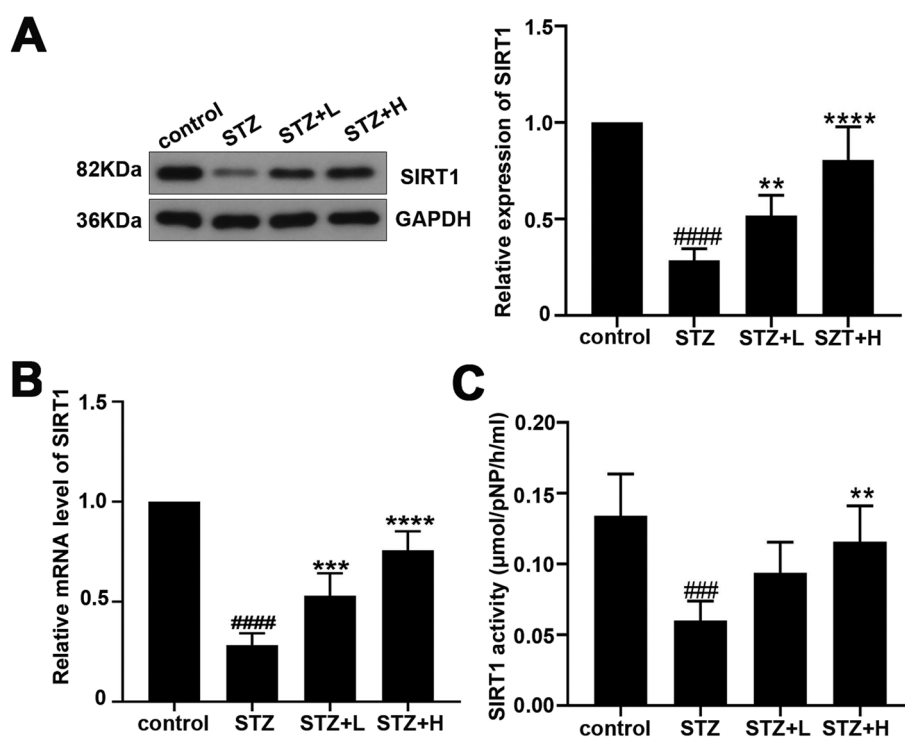


Fig. 4. Schisandrin enhances the activity of SIRT1 in the brain of rats. (A) The protein level of SIRT1 was detected by western-blot. (B) The mRNA level of *Sirt1* was measured by Real-time quantitative PCR. (C) The activity of SIRT1 was tested by an assay kit. Values are expressed as mean \pm SD. n=6. Compared with control group: # P <0.05, ## P <0.01, ### P <0.001, #### P <0.0001; Compared with streptozotocin (STZ) group, * P <0.05, ** P <0.01, *** P <0.001, **** P <0.0001.

gested that neuroinflammatory response in the brain is a significant pathological feature of AD [19]. Our study indicated that schisandrin significantly decreased the expression of these cytokines in a concentration dependent manner which showed the inhibitory effect of schisandrin on inflammation. Furthermore, activation of ER stress response was found along with neuroinflammation. We discovered that expressions of ER stress markers including GRP78, CHOP and cleaved caspase-12 were evidently up-regulated in STZ induced AD rats. The ER stress is mainly caused by the accumulation of unfolded or misfolded protein inside the ER, and excess ER stress response also leads to cell damages [12]. GRP78 is a vital endoplasmic reticulum chaperone which can function in various processes except for ER stress including cell proliferation, protein maturation, folding and transport [17]. CHOP is a key molecule in the downstream of PERK, and ER stress can be mediated by the PERK-CHOP pathway [11]. Caspase-12 is another marker of ER stress which is cleaved into active fragment on ER stress [22]. The augment of these ER stress markers is considered to correlate with increased calcium level and directly destroys the balance of calcium homeostasis which is another important characteristic of AD [5, 12, 16]. Results in our study showed the decrease

in the expression of GRP78, CHOP and cleaved caspase-12 after treatment of schisandrin which indicated the positive effect of schisandrin on ER stress. Astrocytes and microglia are important regulators of inflammatory response in the central nervous system (CNS). Reactive astrocytes and microglia are found in AD and contribute to the progression of Alzheimer's disease [6]. The findings in the present study indicated the potential involvement of astrocyte in the ER stress altered in the STZ-induced AD brain. As we know, CHOP is present in the cytoplasm under non-stressed conditions and ER stress leads to its nuclear accumulation. In our study, GFAP and Iba1 localized in cytoplasm, and some staining of CHOP in nucleus was found to be surrounded with staining of GFAP, but not Iba1, indicating that schisandrin-induced alleviation of ER stress was mainly present in astrocytes.

Sirtuin 1 (SIRT1) is a deacetylase dependent on NAD^+ and has been reported to function in various pathological processes including atherosclerosis, diabetes and cardiomyopathy [26]. Early study finds out that the expression level of SIRT1 in hippocampus is notably reduced in SAMP8 model which has been regarded as a good model for cognitive deficits-related disorders [7]. Furthermore, SIRT1 participates in the regulation of histone

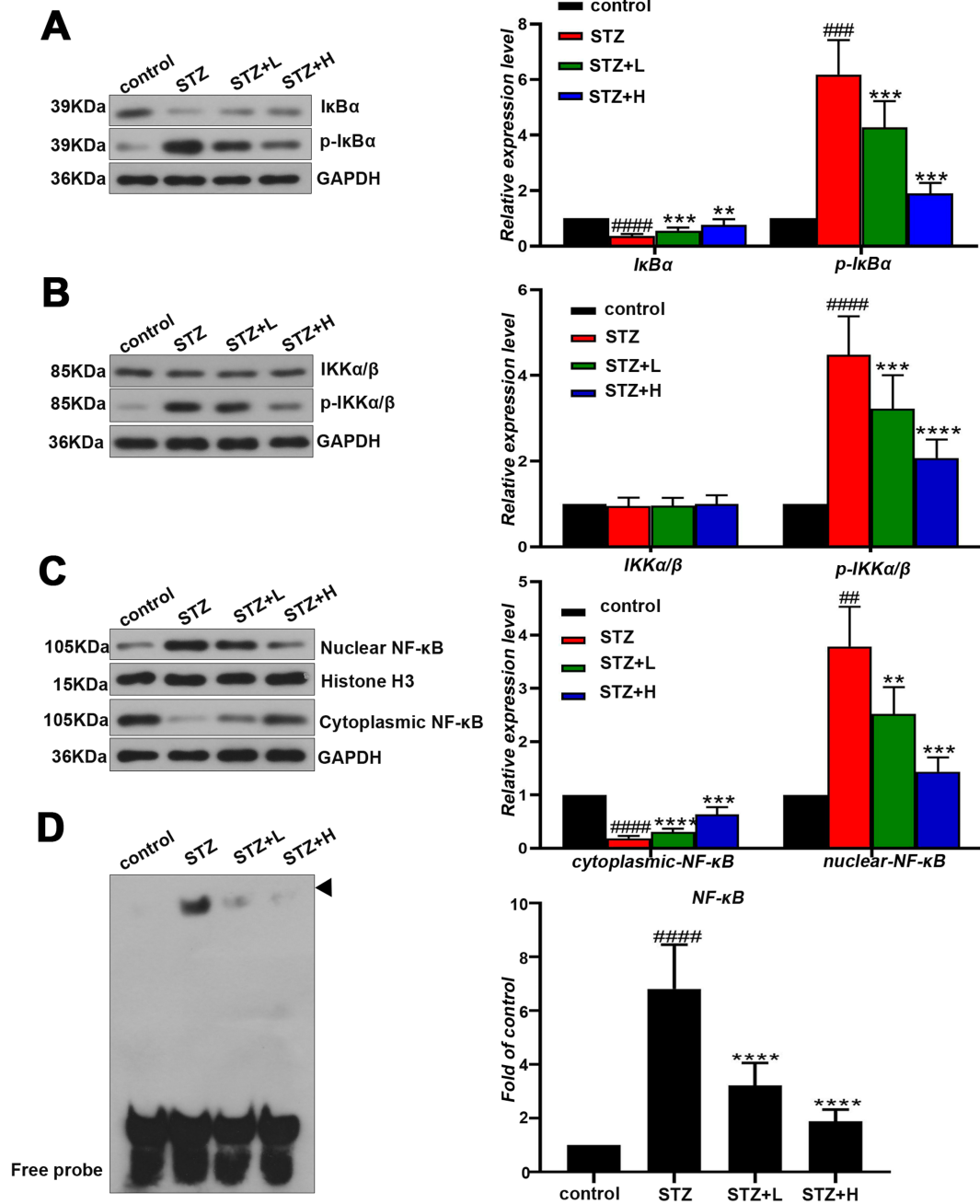


Fig. 5. Schisandrin inhibits the NF- κ B signaling in the brain of rats. The protein levels of I κ B α and p-I κ B α (A); IKK α / β and p-IKK α / β (B) were analyzed by western-blot. (C) The protein levels of NF- κ B extracted from cytoplasm and nucleus were analyzed by western-blot. (D) The activity of NF- κ B-DNA binding was determined by the EMSA. Values are expressed as mean \pm SD. n=6. Compared with control group: # P <0.05, ## P <0.01, ### P <0.001, #### P <0.0001; Compared with streptozotocin (STZ) group, * P <0.05, ** P <0.01, *** P <0.001, **** P <0.0001.

acetylation that has been considered to have an important role in the maintenance and acquisition of memory [7]. SIRT1 has been reported to relieve the ER stress and inflammation [1]. It is demonstrated that SIRT1 may alleviate the ER stress-regulated apoptosis via the decreased expression of CHOP and inactivation of caspase-12 [22]. Moreover, SIRT1 suppresses the ER stress through the mediation of eIF2 α deacetylation [20]. The anti-inflammatory effect of SIRT1 has been confirmed

as attenuation in acetylation of GATA3 and inhibition of Akt/NF- κ B signaling [18]. To fully figure out whether schisandrin mediates SIRT1 to underlie the anti-inflammation and ER stress effects in AD rats, the protein and mRNA levels along with activity of SIRT1 in AD rats with schisandrin treatment were further evaluated. The results indicated that the treatment of schisandrin led to a compensatory activation of SIRT1 in AD rats. Activated SIRT1 has been determined to exert reversal effects

on memory impairment [7, 29]. Additionally, previous studies have demonstrated that schisandrin functions in different process via suppression of NF- κ B pathway. Schisandrin is reported to restrain the cartilage degradation and inflammation by inhibiting the MAPK and NF- κ B pathway [25]. Schisandrin reveals the anti-toxicity through the activation of the Nrf2 pathway and inhibition of MAPKs and NF- κ B pathway [14]. In our study, the degradation of I κ B α and the phosphorylation of I κ B α and IKK α/β in STZ induced group were significantly reversed after schisandrin treatment. Usually, NF- κ B stays in inactive form with the inhibitory protein I κ B. Once the subunit I κ B α activated by cytokines, it is phosphorylated and degraded which leads to the translocation of NF- κ B into nucleus, triggering the downstream gene transcription [9, 15]. The translocation and DNA binding activity of NF- κ B were also remarkably inhibited with schisandrin treatment in our study which indicated that schisandrin negatively regulated the NF- κ B pathway in the brain of AD rats.

Actually, the direct target of schisandrin in AD still remains unclear. Previous study has only indicated that schisandrin mediates the expression of the glycogen synthase kinase (GSK)-3 β , protein kinase B (Akt) and Tau protein in SH-SY5Y cell model of AD, while without the confirmation of the direct target [32]. However, based on the target-network pharmacology strategy, several target genes implicated with AD such as the acetyl cholinesterase, inducible nitric oxide synthase, glycogen synthase kinase 3 β , and hemeoxygenase 1, have been predicted to associate with active ingredients such as schisandrin from *Schisandra chinensis* (Turcz.) Baill [28]. This may provide some references for the investigation on the direct target of schisandrin in AD. In our study, we found out that schisandrin attenuates neuroinflammation and ER stress in STZ-induced AD model. Besides, the up-regulated SIRT1 and alleviation of ER in astrocytes were also revealed after schisandrin treatment. Though targets of schisandrin in AD is particularly complex, our findings still provide novel mechanisms for the neuroprotective effect of schisandrin in AD model.

Conflicts of Interest

The authors declare that they have no conflict of interest.

Acknowledgments

This study was supported by the Professorial and Doctoral of Scientific Research Foundation of Huizhou Uni-

versity (No. 2019JB027), the Scientific Research Foundation of Huizhou Third People's Hospital, and the Scientific Research Project of Heilongjiang Provincial Health and Family Planning Commission (No. 2017-501).

References

1. An, R., Zhao, L., Xu, J., Xi, C., Li, H., Shen, G., Zhang, W., Zhang, S. and Sun, L. 2016. Resveratrol alleviates sepsis-induced myocardial injury in rats by suppressing neutrophil accumulation, the induction of TNF- α and myocardial apoptosis via activation of Sirt1. *Mol. Med. Rep.* 14: 5297–5303. [Medline] [CrossRef]
2. Andruccioli, M.C.D., Matsumoto, M.A.N., Fukada, S.Y., Saraiva, M.C.P., Bergamo, A.Z.N., Romano, F.L., Silva, R.A.B.D., Silva, L.A.B.D. and Nelson-Filho, P. 2019. Quantification of pro-inflammatory cytokines and osteoclastogenesis markers in successful and failed orthodontic mini-implants. *J. Appl. Oral Sci.* 27: e20180476. [Medline] [CrossRef]
3. Angelova, H., Pechlivanova, D., Krumova, E., Miteva-Staleva, J., Kostadinova, N., Dzhabazova, E. and Landzhov, B. 2019. Moderate protective effect of Kyotorphin against the late consequences of intracerebroventricular streptozotocin model of Alzheimer's disease. *Amino Acids* 51: 1501–1513. [Medline]
4. Bassani, T.B., Bonato, J.M., Machado, M.M.F., Cópola-Segovia, V., Moura, E.L.R., Zanata, S.M., Oliveira, R.M.M.W. and Vital, M.A.B.F. 2018. Decrease in Adult Neurogenesis and Neuroinflammation Are Involved in Spatial Memory Impairment in the Streptozotocin-Induced Model of Sporadic Alzheimer's Disease in Rats. *Mol. Neurobiol.* 55: 4280–4296. [Medline]
5. Biswas, J., Gupta, S., Verma, D.K., Gupta, P., Singh, A., Tiwari, S., Goswami, P., Sharma, S. and Singh, S. 2018. Involvement of glucose related energy crisis and endoplasmic reticulum stress: Insinuation of streptozotocin induced Alzheimer's like pathology. *Cell. Signal.* 42: 211–226. [Medline] [CrossRef]
6. Carter, S.F., Herholz, K., Rosa-Neto, P., Pellerin, L., Nordberg, A. and Zimmer, E.R. 2019. Astrocyte Biomarkers in Alzheimer's Disease. *Trends Mol. Med.* 25: 77–95. [Medline] [CrossRef]
7. Diaz-Perdigon, T., Belloch, F.B., Ricobaraza, A., Elboray, E.E., Suzuki, T., Tordera, R.M. and Puerta, E. 2020. Early sirtuin 2 inhibition prevents age-related cognitive decline in a senescence-accelerated mouse model. *Neuropsychopharmacology* 45: 347–357. [Medline] [CrossRef]
8. Du, L.L., Chai, D.M., Zhao, L.N., Li, X.H., Zhang, F.C., Zhang, H.B., Liu, L.B., Wu, K., Liu, R., Wang, J.Z. and Zhou, X.W. 2015. AMPK activation ameliorates Alzheimer's disease-like pathology and spatial memory impairment in a streptozotocin-induced Alzheimer's disease model in rats. *J. Alzheimers Dis.* 43: 775–784. [Medline] [CrossRef]
9. Gray, G.K., McFarland, B.C., Nozell, S.E. and Benveniste, E.N. 2014. NF- κ B and STAT3 in glioblastoma: therapeutic targets coming of age. *Expert Rev. Neurother.* 14: 1293–1306. [Medline] [CrossRef]
10. Hashimoto, S. and Saido, T.C. 2018. Critical review: involvement of endoplasmic reticulum stress in the aetiology of Alzheimer's disease. *Open Biol.* 8: 180024. [Medline] [CrossRef]
11. Hetz, C., and Papa, F.R. 2018. The Unfolded Protein Response and Cell Fate Control. *Mol. Cell* 69: 169–181. [Medline] [CrossRef]
12. Jo, H.J., Yang, J.W., Park, J.H., Choi, E.S., Lim, C.S., Lee, S. and Han, C.Y. 2019. Endoplasmic Reticulum Stress In-

- creases DUSP5 Expression via PERK-CHOP Pathway, Leading to Hepatocyte Death. *Int. J. Mol. Sci.* 20: 4369. [Medline] [CrossRef]
13. Kassab, S., Begley, P., Church, S.J., Rotariu, S.M., Chevalier-Riffard, C., Dowsey, A.W., Phillips, A.M., Zeef, L.A.H., Grayson, B., Neill, J.C., Cooper, G.J.S., Unwin, R.D. and Gardiner, N.J. 2019. Cognitive dysfunction in diabetic rats is prevented by pyridoxamine treatment. A multidisciplinary investigation. *Mol. Metab.* 28: 107–119. [Medline] [CrossRef]
 14. Kim, E.J., Jang, M., Lee, M.J., Choi, J.H., Lee, S.J., Kim, S.K., Jang, D.S. and Cho, I.H. 2017. *Schisandra chinensis* Stem Ameliorates 3-Nitropropionic Acid-Induced Striatal Toxicity via Activation of the Nrf2 Pathway and Inhibition of the MAPKs and NF- κ B Pathways. *Front. Pharmacol.* 8: 673. [Medline] [CrossRef]
 15. Li, R., Dong, Z., Zhuang, X., Liu, R., Yan, F., Chen, Y., Gao, X. and Shi, H. 2019. Salidroside prevents tumor necrosis factor- α -induced vascular inflammation by blocking mitogen-activated protein kinase and NF- κ B signaling activation. *Exp. Ther. Med.* 18: 4137–4143. [Medline]
 16. Liu, P.P., Xie, Y., Meng, X.Y. and Kang, J.S. 2019. History and progress of hypotheses and clinical trials for Alzheimer's disease. *Signal Transduct. Target. Ther.* 4: 29. [Medline] [CrossRef]
 17. Liu, Y., Wang, X., Zhen, Z., Yu, Y., Qiu, Y. and Xiang, W. 2019. GRP78 regulates milk biosynthesis and the proliferation of bovinemammaryepithelial cells through the mTOR signaling pathway. *Cell. Mol. Biol. Lett.* 24: 57. [Medline] [CrossRef]
 18. Ma, K., Lu, N., Zou, F. and Meng, F.Z. 2019. Sirtuins as novel targets in the pathogenesis of airway inflammation in bronchial asthma. *Eur. J. Pharmacol.* 865: 172670. [Medline] [CrossRef]
 19. Mu, R.H., Tan, Y.Z., Fu, L.L., Nazmul Islam, M., Hu, M., Hong, H. and Tang, S.S. 2019. 1-Methylnicotinamide attenuates lipopolysaccharide-induced cognitive deficits via targeting neuroinflammation and neuronal apoptosis. *Int. Immunopharmacol.* 77: 105918. [Medline] [CrossRef]
 20. Prola, A., Pires Da Silva, J., Guilbert, A., Lecru, L., Piquereau, J., Ribeiro, M., Mateo, P., Gressette, M., Fortin, D., Boursier, C., Gallerne, C., Caillard, A., Samuel, J.L., François, H., Sinclair, D.A., Eid, P., Ventura-Clapier, R., Garnier, A. and Lemaire, C. 2017. SIRT1 protects the heart from ER stress-induced cell death through eIF2 α deacetylation. *Cell Death Differ.* 24: 343–356. [Medline] [CrossRef]
 21. Qi, Y., Cheng, X., Jing, H., Yan, T., Xiao, F., Wu, B., Bi, K. and Jia, Y. 2019. Combination of schisandrin and nootkatone exerts neuroprotective effect in Alzheimer's disease mice model. *Metab. Brain Dis.* 34: 1689–1703. [Medline] [CrossRef]
 22. Ren, M.T., Gu, M.L., Zhou, X.X., Yu, M.S., Pan, H.H., Ji, F. and Ding, C.Y. 2019. Sirtuin 1 alleviates endoplasmic reticulum stress-mediated apoptosis of intestinal epithelial cells in ulcerative colitis. *World J. Gastroenterol.* 25: 5800–5813. [Medline] [CrossRef]
 23. Sasaki-Hamada, S., Ikeda, M. and Oka, J.I. 2019. Glucagon-like peptide-2 rescues memory impairments and neuropathological changes in a mouse model of dementia induced by the intracerebroventricular administration of streptozotocin. *Sci. Rep.* 9: 13723. [Medline] [CrossRef]
 24. Sawikr, Y., Yarla, N.S., Peluso, I., Kamal, M.A., Aliev, G. and Bishayee, A. 2017. Neuroinflammation in Alzheimer's Disease: The Preventive and Therapeutic Potential of Polyphenolic Nutraceuticals. *Adv. Protein Chem. Struct. Biol.* 108: 33–57. [Medline] [CrossRef]
 25. Tu, C., Huang, X., Xiao, Y., Song, M., Ma, Y., Yan, J., You, H. and Wu, H. 2019. Schisandrin A Inhibits the IL-1 β -Induced Inflammation and Cartilage Degradation via Suppression of MAPK and NF- κ B Signal Pathways in Rat Chondrocytes. *Front. Pharmacol.* 10: 41. [Medline] [CrossRef]
 26. Wang, Q.L., Yang, L., Peng, Y., Gao, M., Yang, M.S., Xing, W. and Xiao, X.Z. 2019. Ginsenoside Rg1 Regulates SIRT1 to Ameliorate Sepsis-Induced Lung Inflammation and Injury via Inhibiting Endoplasmic Reticulum Stress and Inflammation. *Mediators Inflamm.* 2019: 6453296. [Medline]
 27. Wei, B.B., Liu, M.Y., Chen, Z.X. and Wei, M.J. 2018. Schisandrin ameliorates cognitive impairment and attenuates A β deposition in APP/PS1 transgenic mice: involvement of adjusting neurotransmitters and their metabolite changes in the brain. *Acta Pharmacol. Sin.* 39: 616–625. [Medline] [CrossRef]
 28. Wei, M., Liu, Y., Pi, Z., Li, S., Hu, M., He, Y., Yue, K., Liu, T., Liu, Z., Song, F. and Liu, Z. 2019. Systematically Characterize the Anti-Alzheimer's Disease Mechanism of Lignans from *S. chinensis* based on In-Vivo Ingredient Analysis and Target-Network Pharmacology Strategy by UHPLC-Q-TOF-MS. *Molecules* 24: 1203. [CrossRef]
 29. Wu, S.Y., Liang, J., Yang, B.C. and Leung, P.S. 2019. SIRT1 Activation Promotes β -Cell Regeneration by Activating Endocrine Progenitor Cells via AMPK Signaling-Mediated Fatty Acid Oxidation. *Stem Cells* 37: 1416–1428. [Medline] [CrossRef]
 30. Xu, X., Rajamanicham, V., Xu, S., Liu, Z., Yan, T., Liang, G., Guo, G., Zhou, H. and Wang, Y. 2019. Schisandrin A inhibits triple negative breast cancer cells by regulating Wnt/ER stress signaling pathway. *Biomed. Pharmacother.* 115: 108922. [Medline] [CrossRef]
 31. Yu, Y.Z., Liu, S., Wang, H.C., Shi, D., Xu, Q., Zhou, X.W., Sun, Z.W. and Huang, P.T. 2016. A Novel A β B-Cell Epitope Vaccine (rCV01) for Alzheimer's Disease Improved Synaptic and Cognitive Functions in 3 \times Tg-AD Mice. *J. Neuroimmune Pharmacol.* 11: 657–668. [Medline] [CrossRef]
 32. Zhao, Z.Y., Zhang, Y.Q., Zhang, Y.H., Wei, X.Z., Wang, H., Zhang, M., Yang, Z.J. and Zhang, C.H. 2019. The protective underlying mechanisms of Schisandrin on SH-SY5Y cell model of Alzheimer's disease. *J. Toxicol. Environ. Health A* 82: 1019–1026. [Medline] [CrossRef]
 33. Zhi, Y., Jin, Y., Pan, L., Zhang, A. and Liu, F. 2019. Schisandrin A ameliorates MPTP-induced Parkinson's disease in a mouse model via regulation of brain autophagy. *Arch. Pharm. Res.* 42: 1012–1020. [Medline] [CrossRef]
 34. Zhu, P., Li, J., Fu, X. and Yu, Z. 2019. Schisandra fruits for the management of drug-induced liver injury in China: A review. *Phytomedicine* 59: 152760. [Medline] [CrossRef]